Dynamical heterogeneity in a model for permanent gels: Different behavior of dynamical susceptibilities

T. Abete,[1,2] A. de Candia,[1,2,3] E. Del Gado,[4] A. Fierro,[5] and A. Coniglio[1,3,5]
[1]*Dipartimento di Scienze Fisiche, Università di Napoli "Federico II," Complesso Universitario di Monte Sant'Angelo, via Cintia 80126 Napoli, Italy*
[2]*CNISM Università di Napoli "Federico II," Complesso Universitario di Monte Sant'Angelo, via Cintia 80126 Napoli, Italy*
[3]*INFN Udr di Napoli, Complesso Universitario di Monte Sant'Angelo, via Cintia 80126 Napoli, Italy*
[4]*ETH Zürich, Department of Materials, Polymer Physics, CH-8093 Zürich, Switzerland*
[5]*INFM CNR Coherentia, Complesso Universitario di Monte Sant'Angelo, via Cintia 80126 Napoli, Italy*
(Received 5 August 2008; published 14 October 2008)

We present a systematic study of dynamical heterogeneity in a model for permanent gels upon approaching the gelation threshold. We find that the fluctuations of the self-intermediate scattering function are increasing functions of time, reaching a plateau whose value, at large length scales, coincides with the mean cluster size and diverges at the percolation threshold. Another measure of dynamical heterogeneities—i.e., the fluctuations of the self-overlap—displays instead a peak and decays to zero at long times. The peak, however, also scales as the mean cluster size. Arguments are given for this difference in the long-time behavior. We also find that the non-Gaussian parameter reaches a plateau in the long-time limit. The value of the plateau of the non-Gaussian parameter, which is connected to the fluctuations of diffusivity of clusters, increases with the volume fraction and remains finite at the percolation threshold.

DOI: 10.1103/PhysRevE.78.041404 PACS number(s): 82.70.Dd, 82.70.Gg

I. INTRODUCTION

In the context of the glass transition the concept of dynamical heterogeneities has been very fecund [1–12]. In glassy systems the correlated motion of particles manifests as significant fluctuations around the average dynamics, strongly increasing as the transition is approached. These heterogeneities in the dynamics have been studied quantitatively via the so-called dynamical susceptibility [3] $\chi_4(t)=N[\langle F^2(t)\rangle-\langle F(t)\rangle^2]$, obtained as the fluctuations of a suitable time-dependent correlator $F(t)$ (where N is the number of particles and $\langle\cdots\rangle$ is the ensemble average). Two quantities are usually considered: The fluctuations of the self-intermediate scattering functions (ISFs) [6,13] $\chi_4(k,t)=N[\langle|\Phi_s(k,t)|^2\rangle-\langle\Phi_s(k,t)\rangle^2]$ usually measured in numerical simulations and the fluctuations of the time-dependent overlap [14–16] $\chi_4^Q(t)=N[\langle q(t)^2\rangle-\langle q(t)\rangle^2]$, which, first introduced in p-spin glass models [3], has been calculated also within mode-coupling theory [3,13]. For the fluctuations of the overlap, the role of the inverse of the wave vector k is played by the parameter a characterizing the overlap function, which is different from zero only if a particle has moved a distance less than the fixed value a. In the usual glassy systems the behavior observed in the dynamical susceptibility is essentially the same despite different choices $F(t)$ [4,6,13]: $\chi_4(t)$ grows as a function of time, reaches a maximum, and then decreases to a constant, consistently with the transient nature of the dynamical heterogeneities. Some differences in the k dependence of these two quantities were, however, found in a model for glasses [17].

Recently, dynamical heterogeneities have been studied in other complex systems, such as granular media [18–21] and attractive colloidal systems [22–26], where behaviors qualitatively similar to that found in glasses are observed. In particular, Ref. [26] reports a systematic study of the dynamic susceptibility in colloidal systems along the attractive glassy line. Typically the dynamical susceptibility, defined as the fluctuations of the self-ISF, displays a well-pronounced peak. However, in the attraction-dominated limit, the dependence on both time and wave vector markedly differs from that in standard repulsion-dominated systems (hard-sphere limit).

In a recent Letter [27] we have studied the behavior of the dynamical susceptibility χ_4 defined as the fluctuations of the self-ISF, in a model for permanent gel, where bonds are modeled using a finitely extendable nonlinear elastic (FENE) potential [29,30] between neighboring particles. It was found that the behavior of $\chi_4(k,t)$ is drastically different from that found in glasses. In fact, it grows in time until it reaches a plateau in the limit of large time t, without decaying to 1. The value of the plateau in the limit of low wave vector, $k\to 0$, was in fact found to coincide with the mean cluster size. As a consequence, as the system approaches the gel transition (i.e., the percolation threshold), the value of the plateau diverges. For a fixed value of k, the value of the plateau coincides with the mean cluster size up to a linear size of the order of the inverse of k. Therefore, for any $k>0$ ($k>k_{min}$ in our study), the plateau never diverges: it decreases as k increases and eventually goes to 1.

Here we present a systematic study of this FENE model for permanent gels [27]. Moreover, we compare the behavior of the fluctuations of the self-ISF and of the self-overlap, and find a marked difference between the two. The first one, as mentioned above, is an increasing function of time and tends to a plateau, whereas the second one reaches a maximum and then decreases. However, the value of the maximum scales as the value of the plateau of the fluctuations of the self-ISF, with the same critical exponent of the mean cluster size.

The reason why these two quantities differ so drastically in the long-time limit is the following: the fluctuation of the overlap is related to the correlations between the event that a

monomer has moved a distance less than a in a time interval t and the event that another monomer has also moved a distance less than a in the same interval t. At long time t all particles have moved a distance larger than a and therefore such correlations are zero. On the other hand, in the long-time limit the fluctuation of the self-ISF is related to the correlation of the distance separating monomers i and j at time 0 and the distance between the same monomers at time t. This quantity is different from zero if the particles i and j are in the same cluster.

Although the long-time limit of the two quantities $\chi_4(k,t)$ and $\chi_4^Q(a,t)$ is different in gels with permanent bonds, they have in common not only the property that the plateau and maximum scale in the same way, but also one key feature which is the strong length scale dependence: The peak of the fluctuations of the self-part of the overlap and the plateau of the fluctuations of the self-ISF decrease strongly as the wave vector k (or $1/a$) increases, which is a sign that clusters of bonded particles dominate the dynamics. The same feature is also valid for strong colloidal gels [31]. This strong length scale dependence of the dynamical susceptibility seems to be a distinctive sign of permanent or strong colloidal gelation, compared with the (attractive or repulsive) glass transition.

Finally, we measure the non-Gaussian parameter α_2 and find that, due to the presence of clusters, it is different from zero also in the long-time limit. However, its plateau value, which is connected to diffusivity, remains finite upon approaching the transition.

In Sec. II we introduce the model used and give the details of the numerical simulations. We analyze the self-ISF and its fluctuations in Sec. III and the self-overlap and its fluctuations in Sec. IV. The mean-squared displacement and the non-Gaussian parameter are discussed in Sec. V, whereas Sec. VI contains the concluding remarks. Finally, in the Appendix we investigate the static properties of the sol-gel transition, corresponding to the percolation of permanent bonds between particles [32,33].

II. MODEL AND NUMERICAL SIMULATIONS

We consider a three-dimensional system of N particles interacting with a soft potential given by the Weeks-Chandler-Andersen (WCA) potential [28]

$$U_{ij}^{WCA} = \begin{cases} 4\epsilon\left[(\sigma/r_{ij})^{12} - (\sigma/r_{ij})^6 + \frac{1}{4}\right], & r_{ij} < 2^{1/6}\sigma, \\ 0, & r_{ij} \geqslant 2^{1/6}\sigma, \end{cases} \quad (1)$$

where r_{ij} is the distance between particles i and j

After equilibration, particles less than distant R_0 are linked by adding an attractive potential

$$U_{ij}^{FENE} = \begin{cases} -0.5k_0R_0^2 \ln[1-(r_{ij}/R_0)^2], & r_{ij} < R_0, \\ \infty, & r_{ij} \geqslant R_0, \end{cases} \quad (2)$$

representing a FENE potential, which was first introduced in Ref. [29] and is widely used to study linear polymers [30]. We choose $k_0 = 30\epsilon/\sigma^2$ and $R_0 = 1.5\sigma$ as in Ref. [30] in order to avoid any bond crossing and to use an integration time step Δt not too small [34]. The introduction of the FENE potential leads to the formation of permanent bonds among all the particles whose distance at that time is smaller than R_0.

We have performed molecular dynamics simulations of this model: The equations of motion were solved in the canonical ensemble (with a Nosé-Hoover thermostat) using the velocity-Verlet algorithm [35] with a time step $\Delta t = 0.001\delta\tau$, where $\delta\tau = \sigma(m/\epsilon)^{1/2}$ is the standard unit time for a Lennard-Jones fluid and m is the mass of particle. We use reduced units where the unit length is σ, the unit energy is ϵ, and the Boltzmann constant k_B is set equal to 1. We use periodic boundary conditions and average all the investigated quantities over 32 independent configurations of the system.

The temperature is fixed at $T=2$, and the volume fraction $\phi = \pi\sigma^3 N/6L^3$ (where L is the linear size of the simulation box in units of σ) is varied from $\phi=0.02$ to $\phi=0.12$. Using the percolation approach, we identify the gel phase as the state in which there is a percolating cluster [32,33]. A finite-size scaling analysis is presented in the Appendix, showing that this transition is in the universality class of random percolation. We find that the threshold is $\phi_c = 0.09 \pm 0.01$. In particular, we obtain that the cluster size distribution $n_s \sim s^{-\tau}$ for $\phi = \phi_c$ with $\tau = 2.1 \pm 0.2$, the mean cluster size $S(\phi) = \Sigma s^2 n_s / \Sigma s n_s \sim (\phi_c - \phi)^{-\gamma}$ with $\gamma = 1.8 \pm 0.1$, and the connectedness length $\xi \sim (\phi_c - \phi)^{-\nu}$ with $\nu = 0.88 \pm 0.01$. In the following we fix the number of particles, $N=1000$.

Due to the introduction of bonds, spatial correlations appear at low wave vectors. Although these correlations increase as a function of the volume fraction, the low-k limit of the static structure factor $S(k)$ is always small compared to the number of particles, and no phase separation is observed.

III. SELF-INTERMEDIATE SCATTERING FUNCTION AND ITS FLUCTUATIONS

Relevant information on the relaxation dynamics over different length scales can be obtained from the sel-ISF $F_s(k,t)$:

$$F_s(k,t) = [\langle \Phi_s(k,t) \rangle], \quad (3)$$

where $\langle \cdots \rangle$ is the thermal average over a fixed bond configuration, $[\cdots]$ is the average over 32 independent bond configurations of the system, and

$$\Phi_s(k,t) = \frac{1}{N}\sum_{i=1}^{N} e^{i\vec{k}\cdot[\vec{r}_i(t) - \vec{r}_i(0)]}. \quad (4)$$

In Fig. 1, $F_s(k,t)$ is plotted as a function of t for different ϕ, respectively, for $k_{min} = 2\pi/L \sim 0.35$ (main frame) and $k \sim 7$ (inset). At the smallest wave vector, for very low values of the volume fraction, the self-ISF decays to zero following an exponential behavior. As the volume fraction is increased towards the percolation threshold, we observe the onset of a stretched exponential decay $e^{-(t/\tau)^\beta}$, with β decreasing as a function of ϕ (for instance, $\beta = 0.75 \pm 0.01$ for $\phi = 0.07$ and $\beta = 0.58 \pm 0.02$ for $\phi = 0.085$). The cluster size distribution has started to widen towards the percolation regime (see the Appendix), and therefore, over sufficiently large length scales, the behavior of $F_s(k,t)$ is due to the contribution of different relaxation processes, characterized by different re-

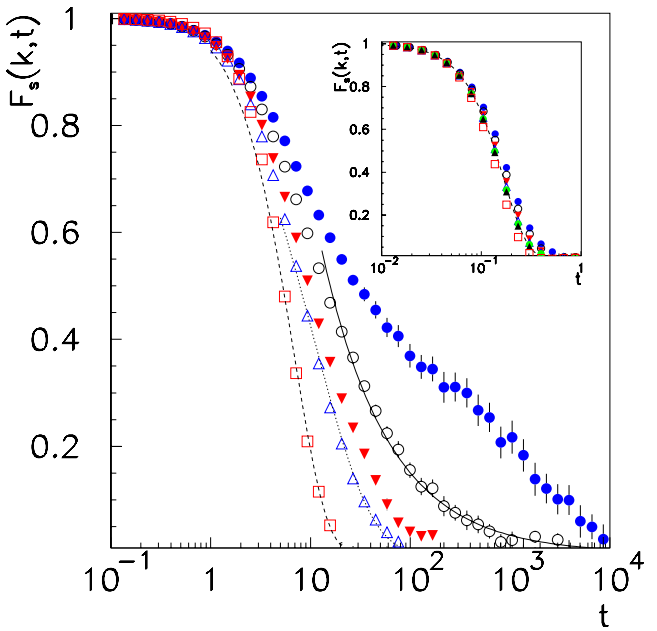

FIG. 1. (Color online) Main frame: self-ISF for $\phi=0.02,0.07,0.08,0.09,0.1$ (from bottom to top) and $k\sim0.35$ as a function of time t. The lines are fitting curves: For $\phi\ll\phi_c$ the decay is well fitted by an exponential behavior (dashed line); if ϕ approaches ϕ_c, a stretched exponential decay appears, with $\beta=0.75\pm0.01$ for $\phi=0.07$ (dotted line). For $\phi=0.09$ the decay is well fitted by a power law $\sim t^{-c}$ with $c=0.65\pm0.03$ (solid line). Inset: self-ISF for $k\sim7$ and the same volume fractions of the main frame.

laxation times, whose superposition produces a detectable deviation from an exponential law. Near the transition threshold the long-time decay is characterized by a power-law behavior, indicating that the relaxation over this length scale is controlled by the formation of the percolating cluster, with a critically growing relaxation time. If the volume fraction increases further, the decay becomes slower and slower, showing a logarithmic behavior. These features of the dynamics well reproduce the experimental findings [36]. Moreover, they agree with results obtained via numerical simulations of different gelation models [37–39]. At large wave vectors (see the inset of Fig. 1) and low volume fractions, $F_s(k,t)$ decays to zero as $e^{-(t/\tau)^2}$ (solid curves in Fig. 1), corresponding to the ballistic regime of particle motion.

From the self-ISF we calculate the structural relaxation time $\tau(k,\phi)$, defined as the time for which $F_s(k,\tau(k))\simeq0.1$. In Fig. 2, $\tau(k,\phi)$ is plotted for different values of k as a function of the volume fraction ϕ. For $k=k_{min}$, we find that $\tau(k_{min},\phi)$ is well fitted by a power law diverging at the gelation threshold with an exponent $f\sim1.22$. Increasing k, no divergence is observed at the threshold, signaling that no structural arrest occurs over length scales less than the box size L.

In Fig. 3 and in its inset we plot, respectively, $k^2\tau(k,\phi)$ and $k\tau(k,\phi)$ as a function of the wave vector for different volume fractions. The inset of Fig. 3 shows that $\tau\sim1/k$ for large wave vectors, reflecting the ballistic diffusion for short times (see Sec. V). Interestingly in the limit of small wave

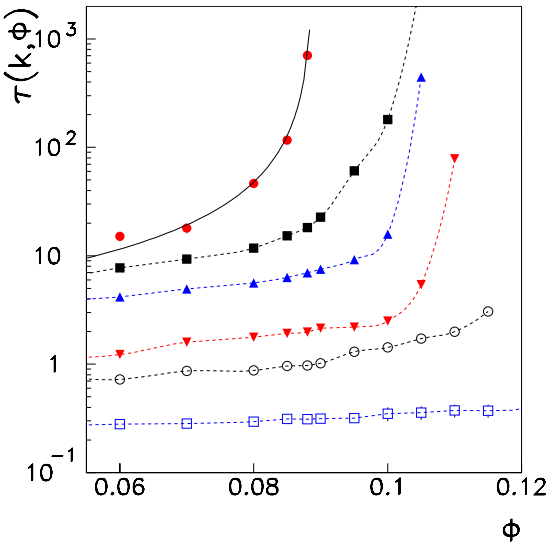

FIG. 2. (Color online) Structural relaxation time $\tau(k,\phi)$ as a function of the volume fraction, for wave vector $k\sim0.35,0.6,1.0,2.0,3.0,7.0$ (from top to bottom). The solid line is the fitting curve: $\tau(k_{min},\phi)\sim(\phi_c-\phi)^{-f}$, with $f\sim1.22$. Dashed lines are guides for the eye.

vectors $k^2\tau$ does not tend to a constant. This unusual result is essentially due to the fact that the the non-Gaussian parameter [40] $\alpha_2(t)=\frac{3\Delta r^4(t)}{5[\Delta r^2(t)]^2}-1$ is nonzero in the long-time limit, as discussed in detail in Sec. V. In this case the Gaussian approximation of the probability distribution of particle displacements is not valid, and the self-ISF $F_s(k,t)$ cannot be written as a Gaussian even in the limit of small wave vector.

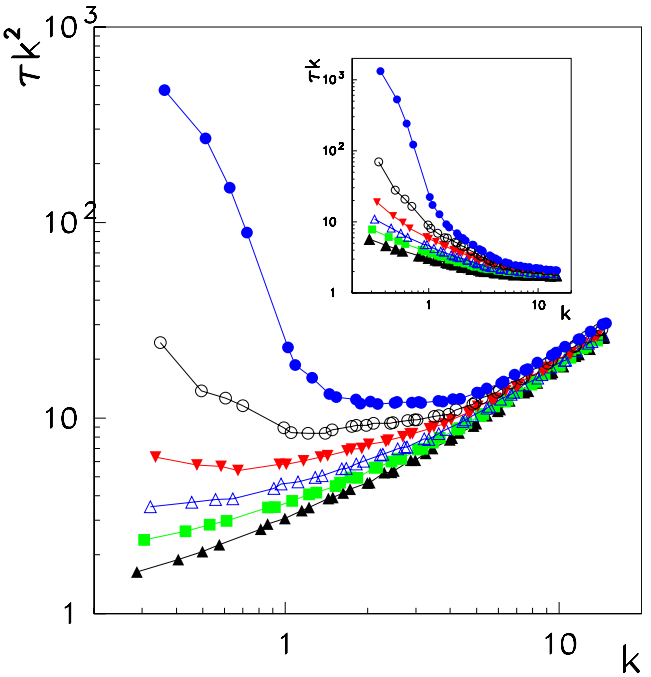

FIG. 3. (Color online) Main frame: $k^2\tau(k,\phi)$ as a function of k, for $\phi=0.05,0.06,0.07,0.08,0.09,0.1$ (from bottom to top). Inset: $k\tau(k,\phi)$ as a function of k for the same volume fractions of the main frame.

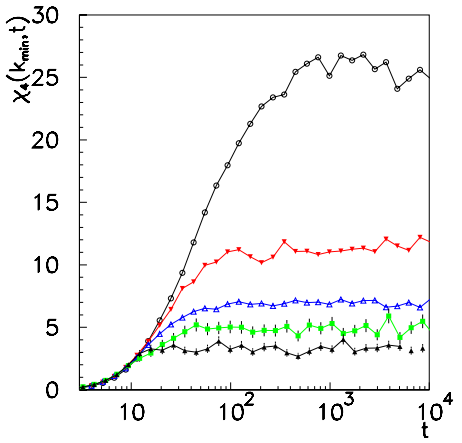

FIG. 4. (Color online) Dynamical susceptibility $\chi_4(k,t)$ as a function of time for $k=k_{min}$ and different volume fractions $\phi=0.05,0.06,0.07,0.08,0.09$ (from bottom to top).

We now analyze and discuss the behavior of the fluctuations of the self-ISF—i.e., the dynamical susceptibility

$$\chi_4(k,t) = N[\langle|\Phi_s(k,t)|^2\rangle - \langle\Phi_s(k,t)\rangle^2]. \tag{5}$$

In Fig. 4 $\chi_4(k,t)$ is plotted for $k=k_{min}$ and different volume fractions. Differently from the behavior typically observed in glassy systems, we find that, for $\phi<\phi_c$, $\chi_4(k,t)$ is a monotonically increasing function of time tending to a plateau in a time of the order of the relaxation time $\tau(k_{min})$. The value of the plateau diverges as the mean cluster size as the percolation threshold is approached [27]. For $\phi\geqslant\phi_c$ the system is out of equilibrium; $\chi_4(k,t)$ continues increasing as a function of time, without reaching any asymptotic value within the simulation time. We briefly discuss the main arguments explaining the above result, presented in Ref. [27], where it was in fact shown that, for $k\to 0$ and $t\to\infty$, the dynamical susceptibility $\chi_4(k,t)$ tends to the mean cluster size. We define $\chi_{as}(k,\phi)\equiv\lim_{N\to\infty}\lim_{t\to\infty}\chi_4(k,t)$. Being $\lim_{t\to\infty}\langle\Phi_s(k,t)\rangle=0$, we have

$$\chi_{as}(k,\phi) = \lim_{N\to\infty}\frac{1}{N}\left[\sum_{i,j=1}^{N} C_{ij}(k)\right], \tag{6}$$

where $C_{ij}(k)=\lim_{t\to\infty}\langle e^{i\vec{k}\cdot[\vec{r}_i(t)-\vec{r}_j(t)]}e^{-i\vec{k}\cdot[\vec{r}_i(0)-\vec{r}_j(0)]}\rangle=|\langle e^{i\vec{k}\cdot(\vec{r}_i-\vec{r}_j)}\rangle|^2$. Here we have used the fact that, for large enough time t, the term $e^{-i\vec{k}\cdot[\vec{r}_i(t)-\vec{r}_j(t)]}$ is statistically independent from $e^{-i\vec{k}\cdot[\vec{r}_i(0)-\vec{r}_j(0)]}$, so that we can factorize the thermal average. We separate the sum over connected pairs ($\gamma_{ij}=1$—i.e., pairs belonging to the same cluster) and disconnected pairs ($\gamma_{ij}=0$—i.e., pairs belonging to different clusters), so that

$$\chi_{as}(k,\phi) = \lim_{N\to\infty}\frac{1}{N}\left[\sum_{i,j=1}^{N}\gamma_{ij}C_{ij}(k)\right] + \frac{1}{N}\left[\sum_{i,j=1}^{N}(1-\gamma_{ij})C_{ij}(k)\right]. \tag{7}$$

If particles i and j are not connected, for any fixed value of $k>0$, the quantity $C_{ij}(k)$ is $O(1/N^2)$ [41]. As there are at most N^2 disconnected pairs, the second term on the night-hand side (rhs) of Eq. (7) is $O(1/N)$ and can be neglected in the thermodynamical limit.

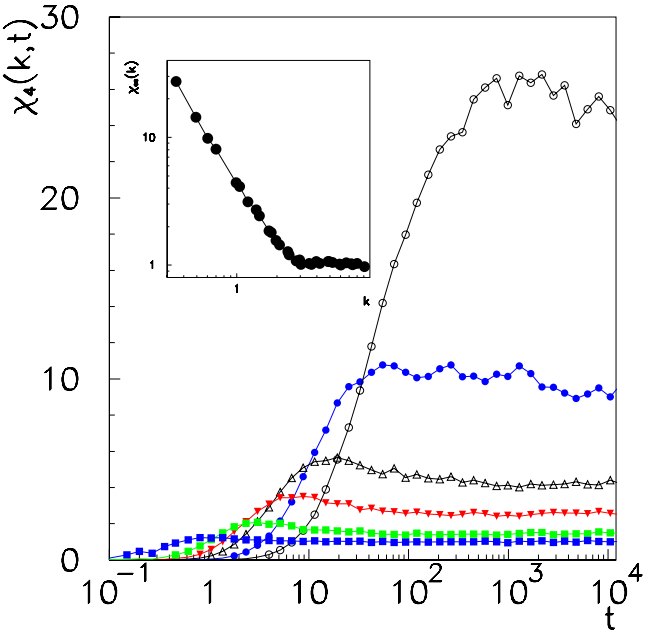

FIG. 5. (Color online) Main frame: dynamical susceptibility $\chi_4(k,t)$ as a function of time for $\phi=0.09$ and $k=0.35,0.61,0.99,1.40,2.10,3.96$ (from top to bottom). Inset: asymptotic values of the susceptibility, $\chi_{as}(k,\phi_c)$, as a function of the wave vector k. Data are fitted with a power law $\sim k^{-2.03\pm0.02}$, in agreement with the exponent $2-\eta$ of random percolation.

For $\phi<\phi_c$, clusters will have at most a linear size of order ξ, so that the relative distance $|\vec{r}_i-\vec{r}_j|$ of connected particles will be smaller than ξ. Therefore we have $\lim_{k\to 0}\gamma_{ij}C_{ij}(k)=\gamma_{ij}$ and

$$\lim_{k\to 0}\chi_{as}(k,\phi) = \lim_{N\to\infty}\frac{1}{N}\left[\sum_{i,j=1}^{N}\gamma_{ij}\right] = S, \tag{8}$$

where S is the mean cluster size. As shown in Ref. [27], numerical data confirm this result.

In Fig. 5, $\chi_4(k,\phi)$ is plotted for $\phi=0.09$ and different wave vectors. For each value of the wave vector, $\chi_4(k,\phi)$ reaches a plateau after a characteristic time of the order of the relaxation time $\tau(k)$. The asymptotic value $\chi_{as}(k,\phi_c)$ at low wave vectors follows a scaling behavior as a function of k (inset of Fig. 5): at the transition threshold the exponent is 2.03 ± 0.02, consistent, within the numerical accuracy, with the prediction $2-\eta$ of random percolation [42]. This result shows that if one varies the wave vector k (and $2\pi/k>\sigma$), the dynamical susceptibility is able to detect the self-similarity of the structure of the system due to the percolation transition. Using scaling arguments [27], we can write $\chi_{as}(k,\phi)=k^{\eta-2}f(k\xi)$, where $f(z)$ is a function, which tends to a constant for small z, whereas it behaves as $z^{\gamma/\nu}$ for large values of z. As shown in Ref. [27], data support this scenario. All these results coherently show how in the present system the asymptotic value of the dynamical susceptibility can be related to the cluster size. Not only do our results indicate that the percolation exponents can be measured in a direct

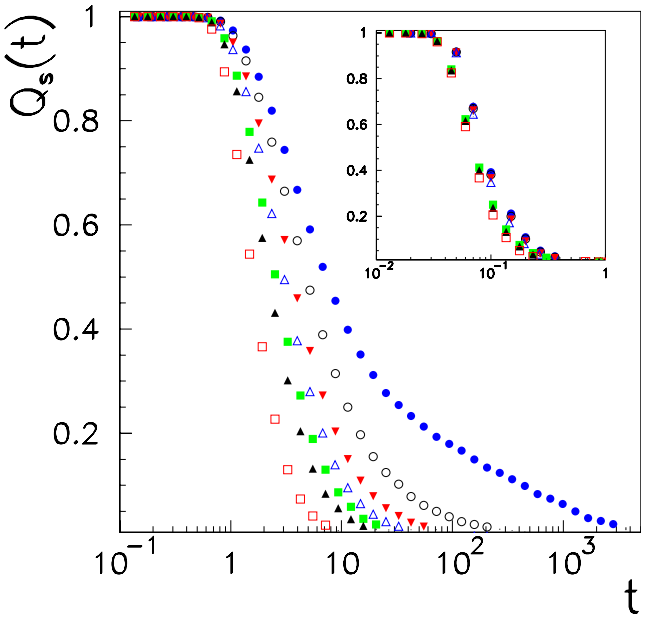

FIG. 6. (Color online) Main frame: Self-overlap $Q_S(t)$ for $a=3$ and different volume fractions from $\phi=0.02,0.05,0.06,0.07,0.08,0.09,0.1$ (from bottom to top). Inset: self-overlap for the same values of ϕ of main frame and $a=0.15$.

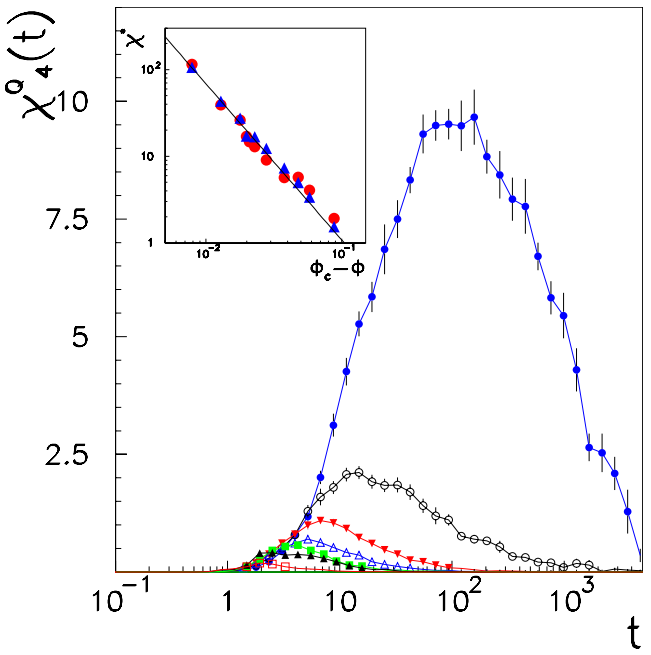

FIG. 7. (Color online) Main frame: fluctuations of the self-overlap $\chi_4^Q(a,t)$ for $a=3$ and $\phi=0.02,0.05,0.06,0.07,0.08,0.09,0.1$ (from bottom to top). Inset: $10\cdot\chi_4^Q(t^*)$ (circles) for $a=3$ and $\chi_{as}(k_{min},\phi)$ (triangles) as a function of $(\phi_c-\phi)$.

way, by developing techniques to measure the dynamical susceptibility, but they also state that the asymptotic value of the dynamical susceptibility plays the same role as the static scattering function near the liquid-gas critical point.

IV. SELF-OVERLAP AND ITS FLUCTUATIONS

In the context of glassy systems, a time-dependent order parameter was introduced [14–16], which measures the number of "overlapping" particles in two configurations separated by a time interval t,

$$q(t)=\frac{1}{N}\int d\vec{r}_1 d\vec{r}_2 \rho(\vec{r}_1,0)\rho(\vec{r}_2,t)w(|\vec{r}_1-\vec{r}_2|)$$

$$=\frac{1}{N}\sum_i\sum_j w(|\vec{r}_i(0)-\vec{r}_j(t)|), \tag{9}$$

where $\rho(\vec{r},t)=\Sigma_i\delta(\vec{r}-\vec{r}_i(t))$ is the density in $\vec{r}$ at time t and $w(|\vec{r}_1-\vec{r}_2|)$ is an "overlap" function that is 1 for $|\vec{r}_1-\vec{r}_2|\leqslant a$ and zero otherwise [43].

In Ref. [4] the authors separate q into self and distinct components, $q(t)=q_S(t)+q_D(t)$. The self part is given by

$$q_S(t)=\frac{1}{N}\sum_i w[|\vec{r}_i(0)-\vec{r}_i(t)|], \tag{10}$$

which corresponds to terms of Eq. (9) with $i=j$ and measures the number of particles that move less than a distance a in a time interval t. In Ref. [4] it was shown that on average the dominant term is given by the self-part.

Here we measure $Q_S(t)=[\langle q_S(t)\rangle]$ for two choices of a, 0.15 and 3, respectively corresponding to $1/a\gg k_{min}$ and $1/a\simeq k_{min}$. $Q_S(t)$ is plotted in Fig. 6 for different values of the volume fraction. We have verified by numerical calculations that for small enough a, the relevant contribution to $Q(t)=[\langle q(t)\rangle]$ is given by $Q_S(t)$, since the probability that a particle replaces within a radius a another particle is small. For all the values of a and of ϕ considered, $Q_S(t)$ at long times is well fitted by a power law.

Another interesting method to investigate the spatially heterogeneous dynamics, generally used in glassy systems, is the measure of the dynamical susceptibility obtained by the fluctuations of the time-dependent overlap [14–16] $\chi_4^Q(a,t)=N[\langle q(t)^2\rangle-\langle q(t)\rangle^2]$, where $q(t)$ is given by Eq. (9). In glassy systems this quantity essentially presents the same features as the fluctuations of the self-ISF.

Here we measure the fluctuations of the self-part of the overlap:

$$\chi_4^Q(a,t)=N[\langle q_S(t)^2\rangle-\langle q_S(t)\rangle^2], \tag{11}$$

for different choices of a, ranging from 0.15 to 3. In Fig. 7 we plot $\chi_4^Q(a,t)$ for $a=3$ and different values of ϕ.

We see that differently from the fluctuations of the self-ISF, here $\chi_4^Q(a,t)$ displays a peak, whose value increases and diverges as the the gel transition is approached. Indeed, the value of the peak differ from the value of the plateau $\chi_{as}(k_{min})$ only for a constant factor (see the inset of Fig. 7) and therefore scales with the same exponent of the mean cluster size γ [44]. Even if the long-time limit of $\chi_4^Q(a,t)$ is strongly different from the one observed in $\chi_4(k,t)$, both fluctuations manifest a strong dependence on the length scale. In fact, the peak of $\chi_4^Q(a,t)$ strongly decreases as a decreases (see Fig. 8). This may be interpreted as a sign that clusters of bonded particle dominate the dynamics.

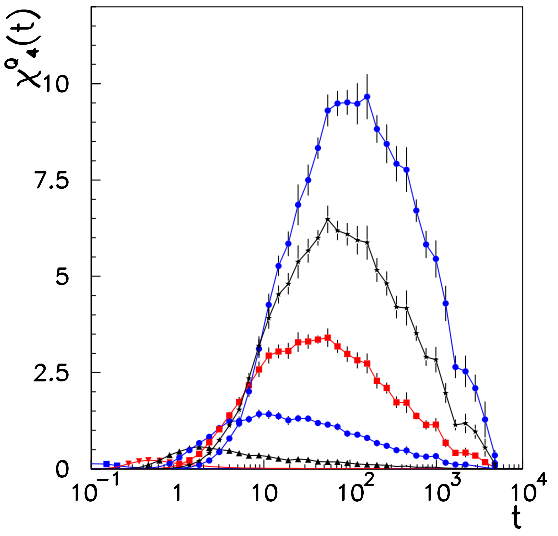

FIG. 8. (Color online) Main frame: fluctuations of the self-overlap $\chi_4^Q(a,t)$ for $\phi=0.1$ and $a=0.15,0.5,1,1.5,2,2.5,3$ (from bottom to top).

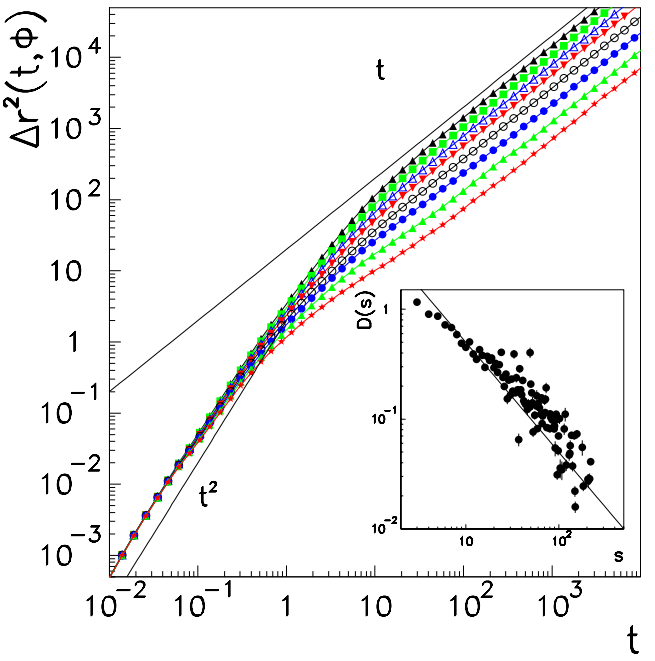

FIG. 9. (Color online) Main frame: mean-square displacement for $\phi=0.05,0.06,0.07,0.08,0.09,0.1,0.11,0.12$. Inset: diffusion coefficient $D(s)$ as a function of the cluster size s for $\phi=\phi_c$.

Our data and these considerations suggest that heterogeneities detected by $\chi_4^Q(a,t)$ are due to the presence of clusters. However, despite the permanent nature of clusters, fluctuations of the self-overlap $\chi_4^Q(a,t)$ decay to zero in the long-time limit. This is due to the form of the overlap function $w[|\vec{r}_i(0)-\vec{r}_i(t)|]$, which is zero when a particle has moved a distance greater than a. Therefore two particles in the same cluster will contribute to $\chi_4^Q(a,t)$ if the center of mass of the cluster has moved a distance less than a. In fact, when the cluster moves a distance larger than a, due to the form of the overlap function, the contribution to $\chi_4^Q(a,t)$ vanishes. Therefore we expect that for $1/a \simeq k_{min}$ the peak is proportional to the mean cluster size and occurs at a time t^* of the order of the time in which the center of the typical cluster of dimension ξ has moved a distance of the order of a.

V. MEAN-SQUARE DISPLACEMENT AND THE NON-GAUSSIAN PARAMETER

Finally we have measured the mean-square displacement (MSD)

$$\Delta r^2(t) = \frac{1}{N}\sum_{i=1}^{N}[\langle|\vec{r}_i(t)-\vec{r}_i(0)|^2\rangle], \tag{12}$$

where $\vec{r}_i(t)$ is the position of the ith particle at time t. In the main frame of Fig. 9 the MSD is shown for different volume fractions. Due to the Newtonian dynamics, we find at very short time a ballistic behavior $\Delta r^2(t) \propto t^2$, followed by a crossover to a diffusive regime $\Delta r^2(t) \propto t$. The long-time diffusive regime is always recovered for all the volume fractions considered, indicating that even at the percolation threshold this quantity is dominated by free motion of particles or clusters. Accordingly, no divergence of the inverse diffusion coefficient is found at the percolation threshold, where the numerous small-size clusters continue to diffuse into the large mesh of the spanning cluster.

We have also evaluated the MSD of the clusters and extracted their diffusion coefficient as a function of the cluster size s. In particular, we obtained that for $\phi=\phi_c$, $D(s)$ for large s is fitted by a power law s^{-h} with $h=1.0\pm0.1$ (see inset of Fig. 9). Following [38] we expect $D(s) \sim 1/s^{(d-2+f/\nu)/d_f}$, where $d=3$ is the Euclidean dimension, f is the exponent which gives the divergence of the viscosity, $\nu \sim 0.88$ is the critical exponent which gives the divergence of the connectedness length (see the Appendix), and $d_f \sim 2.4$ is the fractal dimension of the spanning cluster at the threshold (see the Appendix). Using these values we obtain a prediction for the exponent, which gives the divergence of the viscosity at the threshold $f=\nu(hd_f-d+2) \sim 1.23$, in agreement within the errors with our data for the structural relaxation time (see Sec. III and Fig. 2).

In order to characterize the displacement of particles we have calculated the self-part of the Van Hove function [45]:

$$G_s(r,t) = \frac{1}{N}\left[\left\langle \sum_{i=1}^{N}\delta(r-|\vec{r}_i(t)-\vec{r}_i(0)|)\right\rangle\right]. \tag{13}$$

If the motion of particles is diffusive with a diffusion coefficient D, $G_s(r,t)=(1/4\pi Dt)^{3/2}e^{(-r^2/4Dt)}$, where r is the distance traveled by a particle in a time t. In the inset of Fig. 10 we plot the self Van Hove function for a fixed volume fraction at different times. Our results indicate that for short times and short distances the function is well fitted by a Gaussian. For long distances and long times, the Van Hove function is well fitted by an exponential decay. An exponential decay has been observed in different glassy systems for intermediate times [46].

The deviation from the Gaussian distribution at long times, observed in our system, indicates that some particles

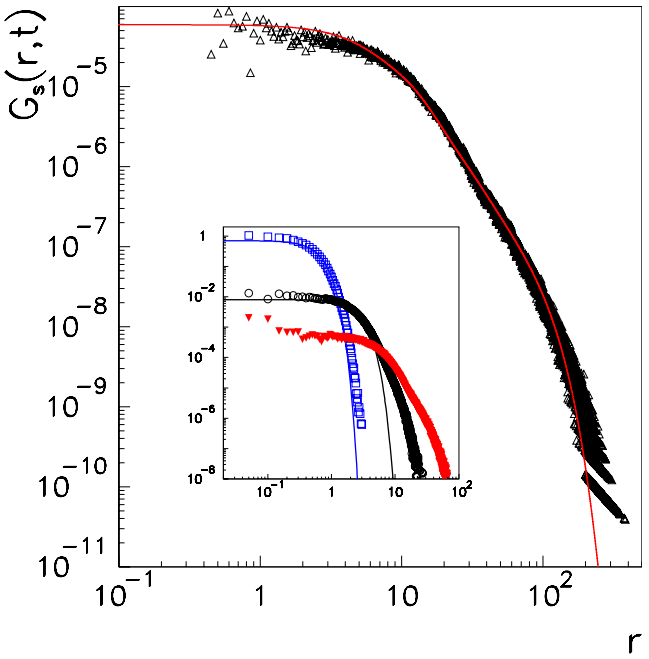

FIG. 10. (Color online) Main frame: the self-part of the Van Hove distribution for $\phi=0.09$ and time $t=1285.02$. The solid line is obtained from the diffusion coefficient of clusters using Eq. (14). Inset: the self-part of the Van Hove distribution for $\phi=0.09$ and different times $t=0.469, 6.739, 93.199$ (from left to right). The lines are Gaussian fitting functions.

move faster than others, due to the presence of clusters. Particles belonging to different clusters have a different diffusion coefficient depending on the cluster size. As a consequence, we suggest that, in the diffusive regime, $G_s(r,t)$ does not have a Gaussian form, but it is instead given by a superposition of Gaussians,

$$G_s(r,t) = \sum_s s n_s \left(\frac{1}{4\pi D(s)t}\right)^{3/2} e^{-r^2/4D(s)t}, \tag{14}$$

where $D(s)$ is the diffusion coefficient of cluster of size s and n_s is the cluster size distribution.

In Fig. 10 we compare our data with $G_s(r,t)$ calculated using Eq. (14) and $D(s)$ obtained from the simulations. As we can see in the figure, data are in good agreement with our predictions, provided that time is sufficiently long for clusters diffusing with diffusion coefficient $D(s)$.

In agreement with this finding, the non-Gaussian parameter, which is a measure of the departure from the Gaussian behavior of the probability distribution of the particle displacements, does not go to zero at long times. The non-Gaussian parameter is defined as [40]

$$\alpha_2(t) = \frac{3\Delta r^4(t)}{5[\Delta r^2(t)]^2} - 1, \tag{15}$$

where $\Delta r^4(t) = \frac{1}{N}\sum_{i=1}^{N}[\langle|\vec{r}_i(t) - \vec{r}_i(0)|^4\rangle]$ and it is zero if the probability distribution of the particle displacements is Gaussian.

In glassy systems [2], (i) on the time scale at which the motion of the particles is ballistic, α_2 is zero; (ii) upon entering the time scale of the β relaxation, α_2 starts to increase; (iii) on the time scale of the α relaxation, α_2 decreases to its long-time limit, zero. The maximum value of α_2 increases with decreasing temperature, signaling that the dynamics becomes more heterogeneous.

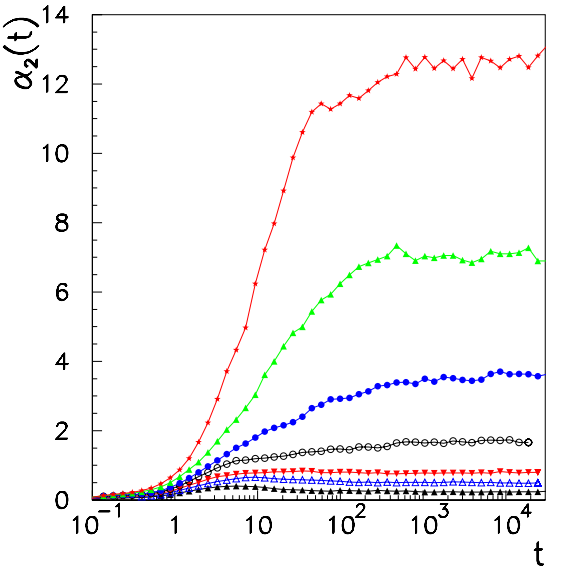

FIG. 11. (Color online) Non-Gaussian parameter $\alpha_2(t)$ as a function of time t for $\phi=0.05, 0.06, 0.07, 0.08, 0.09, 0.1, 0.12$.

In the present model for permanent gels, we find that (i) as in glasses, α_2 is always zero on the time scale at which the motion of the particles is ballistic; (ii) it tends in the long-time limit to a plateau value, which increases with increasing volume fraction; (iii) at low volume fraction, α_2 has a maximum at intermediate times, which disappears upon approaching the gelation threshold; (iv) no critical behavior is observed at the gelation threshold (see Fig. 11).

Within our interpretation the asymptotic value of the non-Gaussian parameter, using Eq. (14) may be written in the following form:

$$\alpha_2^{as} = \frac{\Sigma_s s n_s D^2(s)}{[\Sigma_s s n_s D(s)]^2} - 1 = \frac{\overline{D^2} - \bar{D}^2}{\bar{D}^2}, \tag{16}$$

where, for each bond configuration, $\overline{(\cdots)}$ is the average over the cluster distribution. We have verified that α_2^{as} coincides with $\frac{\overline{D^2}-\bar{D}^2}{\bar{D}^2}$ within the errors. Hence our results indicate that the non-Gaussian parameter tends to a plateau given by the ratio of two quantities, which both have no critical behavior at the percolation threshold. In summary, as the fluctuations of the self-ISF, the non-Gaussian parameter does not decay to zero in the long-time limit, due to the presence of permanent clusters. However, the main contribution to α_2 comes from the numerous finite clusters [the bigger the cluster, the lower its diffusion coefficient $D(s)$, and consequentially its contribution to α_2], so that no criticality approaching the percolation threshold is observed in the non-Gaussian parameter (Fig. 11).

VI. CONCLUSION

We have presented a molecular dynamics study of a model for permanent gels and investigated its static and dynamical properties. Usually the sol-gel transition, marked by the divergence of viscosity and the onset of an elastic modulus, is interpreted in terms of the appearance of a percolating cluster of monomers linked by bonds [32,33,42]. While the viscosity and the elastic modulus can be measured directly, usually the experimental determination of percolative properties needs the manipulation of the sample (for a review see [47] and references therein); i.e. the sample is dissolved in a known quantity of solvent in such a way that each cluster is separated from the others. Our results identify the thermodynamical observable associated with the cluster properties in a gelling system and, via the measure of the fluctuations of the self-ISF, allow us to obtain the critical exponents without such a manipulation of the sample.

In our model the formation of permanent bonds between the particles leads to a percolation transition in the universality class of random percolation. The percolation threshold coincides with the gelation threshold, marked by the slowing down of dynamics on length scale of the whole system. We have found that the behavior of the self-ISF in the sol phase and near the threshold is in agreement with typical experiments on gelling systems. In chemical gels the onset of a stretched exponential decay is typically associated to the wide cluster size distribution close to the gelation threshold, producing a wide distribution of relaxation times. At the percolation threshold, the longest relaxation time diverges due to the critical growing of the percolation correlation length, producing a long-time power-law decay. Our results confirm this picture, but new insights are obtained with a study of the dynamical heterogeneities, in terms of fluctuations of different correlation functions. In the present model for permanent gels, the fluctuations of the self-overlap present always a peak, whereas the fluctuations of the self-ISF are monotonically increasing with time. Differently from glassy systems, the fluctuations of the self-ISF tend in the long-time limit to a plateau, whose value, for the lowest wave vector, coincides with the mean cluster size. The behavior of the non-Gaussian parameter as a function of time is qualitatively similar: in the long-time limit it reaches a plateau, due to the contribution of particles belonging to different clusters with a size-dependent diffusion coefficient. Nevertheless, the value of the plateau does not diverge at the gelation transition, being dominated by the presence of small clusters with finite diffusivity.

This study has shed some light on the differences between the dynamics and the dynamical heterogeneities in glasses and chemical gels. We have been able to clarify that, when clusters of bonded particles are present, different time correlators can deliver very different information whereas in the studies on glasses they are often used interchangeably. On this basis, these findings have interesting implications for the study of gels due to nonpermanent bonds, as in the case of colloidal gels. In fact, our study also indicates a possible way to discriminate between a gel-like behavior and a glass-like behavior in these systems. Our results strongly suggest that, if heterogeneities are due to clusters of particles connected by permanent (or persistent) bonds, as in permanent (or colloidal) gels, the behavior of the "time-dependent order parameter," whose fluctuations reveal the presence of heterogeneities in the dynamics, may be quite different. However, both quantities show a strong length scale dependence (both strongly decrease as k or $1/a$ increase), which seems to be the distinct sign of (permanent or colloidal) gelation compared with the (attractive or repulsive) glass transition [31]. This result is confirmed by a recent work [48], where it has been found that, in a model for colloidal gels, at low volume fraction, the fluctuations of the self-ISF for small wave vector display a dependence on time, which is dramatically different from the one found at higher volume fraction [23,26] in the glassy regime. As a final remark, it is interesting to note that in the model here discussed the dynamical susceptibility is similar to that observed in a spin glass model with quenched interactions [49], suggesting a possible common description of the phase transition involved, as also proposed elsewhere [50].

ACKNOWLEDGMENTS

The research was supported by the EU Network No. MRTN-CT-2003-504712, INFM-PCI, and S.Co.P.E.

APPENDIX: PERCOLATION TRANSITION

In this appendix, with a finite-size scaling analysis, the percolation threshold and the critical exponents are obtained. We find that the percolation of permanent bonds, corresponding to the sol-gel transition [32,33], is in the universality class of random percolation.

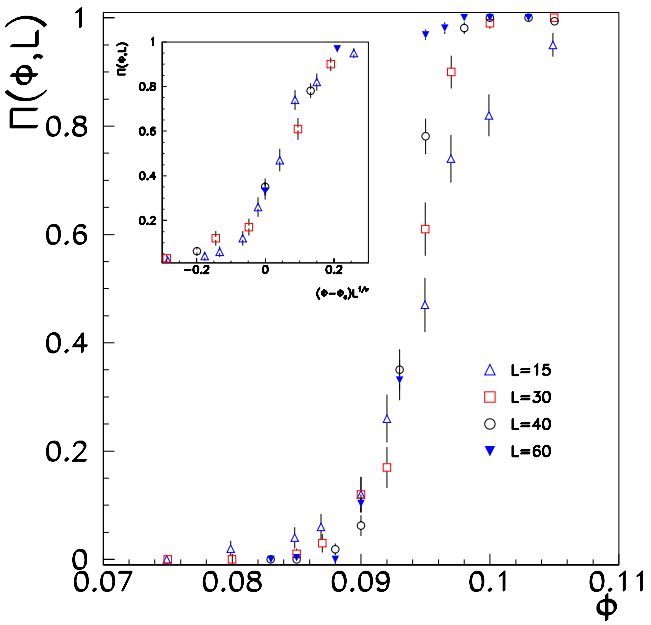

FIG. 12. (Color online) Main frame: percolation probability $\Pi(\phi,L)$ as a function of the volume fraction ϕ for boxes of size $L=15,30,40,60$. Inset: data collapse obtained plotting $\Pi(\phi,L)$ versus $(\phi-\phi_c)L^{1/\nu}$ with $\nu=0.88$ and $\phi_c=0.09$.

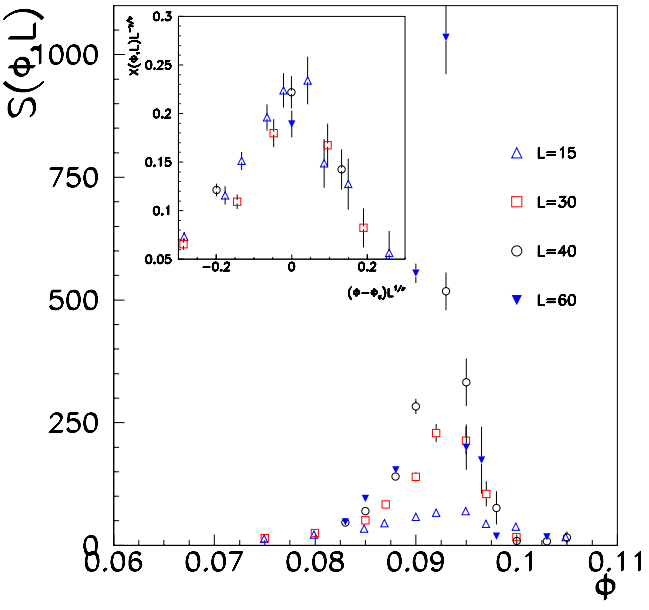

FIG. 13. (Color online) Main frame: mean cluster size $S(\phi,L)$ as a function of the volume fraction ϕ for boxes of the same sizes of Fig. 12. Inset: data collapse obtained plotting $S(\phi,L)L^{-\gamma/\nu}$ versus $(\phi-\phi_c)L^{1/\nu}$ with $\nu=0.88$, $\phi_c=0.09$, and $\gamma=1.85$.

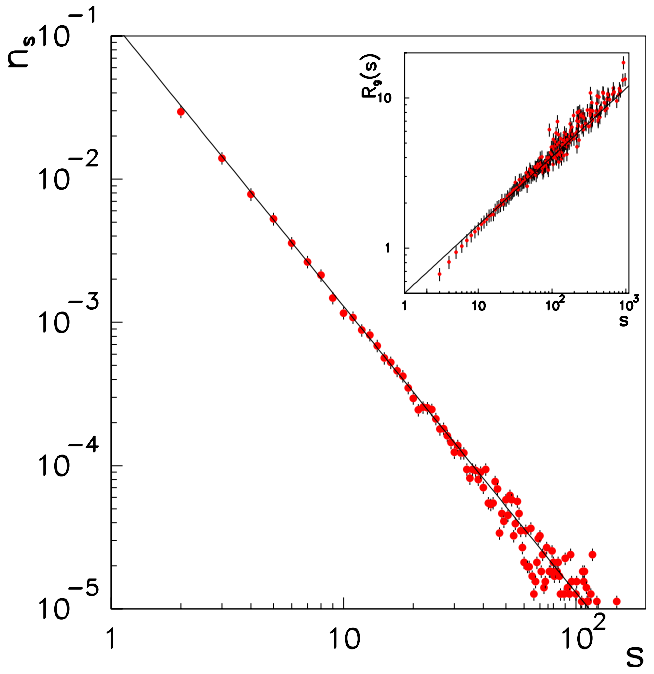

FIG. 14. (Color online) Main frame: average number of clusters (per particle) with mass s versus s at ϕ_c for $L=40$. The solid line is a power law $s^{-\tau}$ with fitting parameter $\tau=2.1$. Inset: radius of gyration, R_g, as a function of the mass s of clusters at ϕ_c for $L=40$. The solid line is a power law s^{1/d_f} with fitting parameter $d_f=2.4$.

Varying the volume fraction ϕ, we have measured the percolation probability $\Pi(\phi)$ (defined as the average number of configurations where a percolating cluster is found), the cluster size distribution n_s, and the mean cluster size $S(\phi)=\Sigma s^2 n_s/\Sigma s n_s$. For each volume fraction we have used simulation boxes of different size L and, from a standard finite-size scaling analysis [42], we have obtained the percolation threshold ϕ_c and the critical exponents ν (which governs the power-law divergence of the connectedness length $\xi\sim|\phi-\phi_c|^{-\nu}$ as the transition threshold is approached from below) and γ (which governs the power-law divergence of the mean cluster size $S\sim|\phi-\phi_c|^{-\gamma}$). The percolation threshold and the critical exponents obtained from the data shown in Figs. 12 and 13 are, respectively, $\phi_c=0.09\pm0.01$, $\nu=0.88\pm0.05$, and $\gamma=1.85\pm0.05$. The cluster size distribution n_s for $\phi=\phi_c$, shown in main frame of Fig. 14, follows a power-law behavior $n_s\sim s^{-\tau}$ with a Fisher exponent $\tau=2.1\pm0.2$.

Finally in the inset of Fig. 14 the radius of gyration, R_g, as a function of the mass s of clusters is plotted. The data are well fitted by a power law with exponent $1/d_f=0.42\pm0.03$ (solid line in figure), which gives $d_f=2.4\pm0.1$, in agreement with the fractal dimension of the random percolation clusters in 3D, $d_f\simeq2.5$. The measured values of the critical exponents satisfy the hyperscaling relations [$2\beta+\gamma=\nu d$, $d_f=d-\beta/\nu$, and $\tau=2+(d-d_f)/d_f$ [42]] and are in good agreement with those of the 3D random percolation ($\nu=0.88$, $\gamma=1.80$, and $\tau=2.18$ [42]).

[1] M. T. Cicerone, F. R. Blackburn, and M. D. Ediger, Macromolecules **28**, 8224 (1995); M. T. Cicerone and M. D. Ediger, J. Chem. Phys. **104**, 7210 (1996).
[2] W. Kob, C. Donati, S. J. Plimpton, P. H. Poole, and S. C. Glotzer, Phys. Rev. Lett. **79**, 2827 (1997).
[3] S. Franz and G. Parisi, J. Phys.: Condens. Matter **12**, 6335 (2000).
[4] N. Lacevic, F. W. Starr, T. B. Schroder, and S. C. Glotzer, J. Chem. Phys. **119**, 7372 (2003).
[5] C. Bennemann, C. Donati, J. Baschnagel, and S. C. Glotzer, Nature (London) **399**, 246 (1999).
[6] L. Berthier, G. Biroli, J.-P. Bouchaud, L. Cipelletti, D. El Masri, D. L'Hôte, F. Ladieu, and M. Pierno, Science **310**, 1797 (2005).
[7] A. Widmer-Cooper, P. Harrowell, and H. Fynewever, Phys. Rev. Lett. **93**, 135701 (2004).
[8] J.-P. Bouchaud and G. Biroli, Phys. Rev. B **72**, 064204 (2005).
[9] G. Biroli, J.-P Bouchaud, K. Miyazaki, and D. R. Reichman, Phys. Rev. Lett. **97**, 195701 (2006).
[10] L. Berthier, G. Biroli, J-P Bouchaud, W. Kob, K. Miyazaki, and D. R. Reichman, J. Chem. Phys. **126**, 184503 (2007); **126**, 184504 (2007).
[11] P. Chaudhuri, L. Berthier, and W. Kob, Phys. Rev. Lett. **99**, 060604 (2007).
[12] C. Dalle-Ferrier, C. Thibierge, C. Alba-Simionesco, L. Berthier, G. Biroli, J.-P. Bouchaud, F. Ladieu, D. L'Hote, and G. Tarjus, Phys. Rev. E **76**, 041510 (2007).
[13] G. Biroli and J. P. Bouchaud, Europhys. Lett. **67**, 21 (2004); C. Toninelli, M. Wyart, L. Berthier, G. Biroli, and J.-P. Bouchaud, Phys. Rev. E **71**, 041505 (2005).

[14] S. Franz, C. Donati, G. Parisi, and S. C. Glotzer, Philos. Mag. B **79**, 1827 (1999); C. Donati, S. Franz, S. C. Glotzer, and G. Parisi, J. Non-Cryst. Solids **307**, 215 (2002).

[15] S. C. Glotzer, V. N. Novikov, and T. B. Schroder, J. Chem. Phys. **112**, 509 (2000).

[16] N. Lacevic, F. W. Starr, T. B. Schroder, V. N. Novikov, and S. C. Glotzer, Phys. Rev. E **66**, 030101(R) (2002).

[17] D. Chandler, J. P. Garrahan, R. L. Jack, L. Maibaum, and A. C. Pan, Phys. Rev. E **74**, 051501 (2006).

[18] A. Fierro, M. Nicodemi, M. Tarzia, A. de Candia, and A. Coniglio, Phys. Rev. E **71**, 061305 (2005).

[19] A. Lefevre, L. Berthier, and R. Stinchcombe, Phys. Rev. E **72**, 010301(R) (2005).

[20] O. Dauchot, G. Marty, and G. Biroli, Phys. Rev. Lett. **95**, 265701 (2005).

[21] A. S. Keys, A. R. Abate, S. C. Glotzer, and D. J. Durian, Nat. Phys. **3**, 260 (2007).

[22] E. Weeks, J. C. Crocker, A. C. Levitt, A. Schofield, and D. A. Weitz, Science **287**, 627 (2000); E. R. Weeks and D. A. Weitz, Phys. Rev. Lett. **89**, 095704 (2002).

[23] L. Cipelletti and L. Ramos, J. Phys.: Condens. Matter **17**, R253 (2005); A. Duri, H. Bissig, V. Trappe, and L. Cipelletti, Phys. Rev. E **72**, 051401 (2005); A. Duri and L. Cipelletti, Europhys. Lett. **76**, 972 (2006).

[24] D. R. Reichman, E. Rabani, and P. L. Geissler, J. Phys. Chem. B **109**, 14654 (2005).

[25] A. M. Puertas, M. Fuchs, and M. E. Cates, Phys. Rev. E **67**, 031406 (2003); J. Chem. Phys. **121**, 2813 (2004); J. Phys. Chem. B **109**, 6666 (2005).

[26] P. Charbonneau and D. R. Reichman, Phys. Rev. Lett. **99**, 135701 (2007).

[27] T. Abete, A. de Candia, E. Del Gado, A. Fierro, and A. Coniglio, Phys. Rev. Lett. **98**, 088301 (2007).

[28] J. D. Weeks, D. Chandler, and H. C. Andersen, J. Chem. Phys. **54**, 5237 (1971).

[29] H. R. Warner, Ind. Eng. Chem. Fundam. **11**, 379 (1972).

[30] K. Kremer and G. S. Grest, J. Chem. Phys. **92**, 5057 (1990); **94**, 4103(E) (1991); G. S. Grest and K. Kremer, Macromolecules **20**, 1376 (1987); Phys. Rev. A **33**, 3628 (1986); M. Murat and G. S. Grest, Phys. Rev. Lett. **63**, 1074 (1989).

[31] A. de Candia, E. Del Gado, A. Fierro, and A. Coniglio (unpublished).

[32] P. J. Flory, *The Physics of Polymer Chemistry* (Cornell University Press, Ithaca, NY, 1954).

[33] P. G. de Gennes, *Scaling Concepts in Polymer Physics* (Cornell University Press, Ithaca, NY, 1993).

[34] Increasing k would reduce the maximum extension further, but would require a reduction in Δt.

[35] S. Nosé, J. Chem. Phys. **81**, 511 (1984); W. G. Hoover, Phys. Rev. A **31**, 1695 (1985); M. P. Allen and D. J. Tildsley, *Computer Simulation of Liquids* (Oxford University Press, Oxford, 2000).

[36] J. E. Martin, J. Wilcoxon, and D. Adolf, Phys. Rev. A **36**, 1803 (1987); J. E. Martin and J. P. Wilcoxon, Phys. Rev. Lett. **61**, 373 (1988); J. E. Martin, J. P. Wilcoxon, and J. Odinek, Phys. Rev. A **43**, 858 (1991); P. Lang and W. Burchard, Macromolecules **24**, 815 (1991). S. Z. Ren and C. M. Sorensen, Phys. Rev. Lett. **70**, 1727 (1993); F. Ikkai and M. Shibayama, Phys. Rev. Lett. **82**, 4946 (1999).

[37] E. Del Gado, A. Fierro, L. de Arcangelis, and A. Coniglio, Phys. Rev. E **69**, 051103 (2004).

[38] E. Del Gado, L. de Arcangelis, and A. Coniglio, Eur. Phys. J. E **2**, 359 (2000).

[39] I. Saika-Voivod, E. Zaccarelli, F. Sciortino, S. V. Buldyrev, and P. Tartaglia, Phys. Rev. E **70**, 041401 (2004).

[40] A. Rahman, K. S. Singwi, and A. Sjolander, Phys. Rev. **136**, A405 (1964).

[41] We can write

$$\langle e^{-i\vec{k}\cdot(\vec{r}_i-\vec{r}_j)}\rangle = \frac{1}{N}\int d^3\vec{r} e^{-i\vec{k}\cdot\vec{r}}\rho[h_{ij}(\vec{r})+1], \tag{A1}$$

where $\rho=N/V$, $h_{ij}(\vec{r})+1=g_{ij}(\vec{r})$, and $(1/V)g_{ij}(\vec{r})$ gives the probability density of finding the particle i in $\vec{r}$, given the particle j in the origin. For disconnected pairs, in the thermodynamic limit ($N\to\infty$ and $L\to\infty$ leaving the density ρ constant) the integral in Eq. (A1) remains finite for any finite fixed k, so that the left-hand side (lhs) of Eq. (A1) is $O(1/N)$. In fact, the first term, the Fourier transform of the correlation function $h_{ij}(\vec{r})$, is finite when $L\to\infty$ since $h_{ij}(\vec{r})$ decays to zero at a finite distance. The second term, the modulus of the Fourier transform of 1, is not larger than $8/|k_xk_yk_z|$ and consequently remains finite when $L\to\infty$. The quantity $C_{ij}(k)$, being the square modulus of the lhs of Eq. (A1), is therefore $O(1/N^2)$.

[42] D. Stauffer and A. Aharony, *Introduction to Percolation Theory* (Taylor & Francis, London, 1992).

[43] In the simulations this is implemented by choosing $\omega(r)=a^{12}/(a^{12}+r^{12})$. In glassy systems the parameter a is usually chosen ~ 0.3. The reasons of this choice are discussed in Ref. [4].

[44] Neglecting the correlation between particles belonging to different clusters and supposing that the displacement of each cluster at the time t depends only on its size s, $\chi_4^Q(a,t)$ can be written for long enough times in the following way:

$$\chi_4^Q(a,t) \sim \sum_s n_s s^2\{\langle w^2[r_{CM}(s,t)]\rangle - \langle w[r_{CM}(s,t)]\rangle^2\},$$

where $r_{CM}(s,t)$ is the displacement of any cluster of size s at the time t. In principle, $f(s,t)=\langle w^2[r_{CM}(s,t)]\rangle - \langle w[r_{CM}(s,t)]\rangle^2$ depends on the cluster size s. If $f(t,s)$, for a given a, displays, at a time t^*, a peak whose value does not depend on the cluster size s, we obtain that $\chi_4^Q(t^*)$ is proportional to the mean cluster size.

[45] J.-P. Hansen and I. R. McDonald, *Theory of Simple Liquids*, 2nd ed. (Academic, London, 1986).

[46] D. A. Stariolo and G. Fabricius, J. Chem. Phys. **125**, 064505 (2006); P. I. Hurtado, L. Berthier, and W. Kob, Phys. Rev. Lett. **98**, 135503 (2007); P. Chaudhuri, L. Berthier, and W. Kob, *ibid.* **99**, 060604 (2007).

[47] D. Stauffer, A. Coniglio, and M. Adam, Adv. Polym. Sci. **44**, 103 (1982).

[48] A. Fierro, A. de Candia, E. Del Gado, and A. Coniglio, J. Stat. Mech.: Theory Exp. (2008), L04002.

[49] A. Fierro, A. de Candia, and A. Coniglio, Phys. Rev. E **62**, 7715 (2000).

[50] P. M. Goldbart, H. E. Castillo, and A. Zippelius, Adv. Phys. **45**, 393 (1996); C. Wald, P. M. Goldbart, and A. Zippelius, J. Chem. Phys. **124**, 214905 (2006).